Bridging Gold: B-Au-B Three-Center-Two-Electron Bonds in Electron-Deficient $B_2Au_n^{-/0}$ ($n = 1, 3, 5$) and Mixed Analogues

WEN-ZHI YAO,[1] DA-ZHI LI,[1] SI-DIAN LI[1,2]

[1]*Institue of Molecular Science, Shanxi University, Taiyuan 030001, Shanxi, People's Republic of China*

[2]*Institute of Materials sciences and Department of Chemistry, Xinzhou Teachers' University, Xinzhou 034000, Shanxi, People's Republic of China*

Received 7 January 2010; Revised 10 May 2010; Accepted 12 May 2010

DOI 10.1002/jcc.21602

Published online 22 July 2010 in Wiley Online Library (wileyonlinelibrary.com).

Abstract: A systematic density functional theory and wave function theory investigation on the geometrical and electronic structures of the electron-deficient diboron aurides $B_2Au_n^{-/0}$ ($n = 1, 3, 5$) and their mixed analogues $B_2H_mAu_n^-$ ($m + n = 3, 5$) has been performed in this work. *Ab initio* theoretical evidences strongly suggest that bridging gold atoms exist in the ground states of C_{2v} B_2Au^-($^1A_1$), C_2 $B_2Au_3^-$(^1A), C_{2v} B_2Au_3($^2B_1$), C_{2v} $B_2Au_5^-$($^1A_1$), and C_s B_2Au_5($^2A''$), which all prove to possess a B—Au—B three-center-two-electron (3c-2e) bond. For $B_2H_mAu_n^-$ ($m + n = 3, 5$) mixed anions, bridging B—Au—B units appear to be favored in energy over bridging B—H—B, as demonstrated by the fact that the Au-bridged C_{2v} $B_2H_2Au^-$ ($^1A_1$), C_s $B_2HAu_2^-$ ($^1A'$), and C_1 $B_2HAu_4^-$ (^1A) lie clearly lower than their H-bridged counterparts C_s $B_2H_2Au^-$ ($^1A'$), C_2 $B_2HAu_2^-$ (^1A), and C_{2v} $B_2HAu_4^-$ ($^1A_1$), respectively. Orbital analyses indicate that Au 6s makes about 92–96% contribution to the Au-based orbitals in these B-Au-B 3c-2e interactions, whereas Au 5d contributes 8–4%. The adiabatic and vertical detachment energies of the concerned anions have been calculated to facilitate their future experimental characterizations. The results obtained in this work establish an interesting 3c-2e bonding model (B—Au—B) for electron-deficient systems in which Au 6s plays a major role with non-negligible contribution from Au 5d.

 J Comput Chem 32: 218–225, 2011

Key words: diboron aurides; bridging gold; 3c-2e bonds; *ab initio* calculations; structures; properties

Introduction

Gold differs dramatically from other coinage metals (Cu and Ag) mainly because of its strong relativistic effects: the stabilization and contraction of Au 6s and the concomitant destabilization and expansion of Au 5d.[1,2] This gives rise to the high-electronic affinity of Au that behaves like halogens in alkaline metal and transition metal aurides.[1–4] Au also possesses the highest electronegativity (2.4) in all metals, which is comparable with that of H (2.2). Au/H similarity is well supported by the surprising experimental discovery of H/$AuPR_3$ analogy[5] and, more recently, the joint experimental and theoretical confirmation of the H/Au isolobal relationship in silicon aurides T_d $SiAu_4^{0/-}$,[6] C_{2v} $Si_2Au_2^{0/-}$, and C_{2h}/C_{2v} $Si_2Au_4^-$[7] and heptaboron auride C_{2v} $B_7Au_2^{0/-}$.[8] Cage-like $B_nAu_n^{2-}$ ($n = 5$–12) with n-Au terminals were predicted stable recently in theory.[9] Relativistic pseudopotential calculations on the X-centered XAu_n^{m+} cluster cations (X = B—N, Al—S, $n = 4$–6)[10] and Au-bridged X···Au-Y Lewis acid-base pairs[11] were also reported. However, to the best of our knowledge, there have been no investigations reported in literature on bridging gold atoms in electron-deficient systems possessing three-center two-electron (3c-2e) bonds. In this work, we choose diboron aurides $B_2Au_n^{-/0}$ ($n = 1, 3, 5$) and their mixed analogues $B_2H_mAu_n^-$ ($m + n = 3, 5$) as typical examples to investigate the possibility of electron-deficient B-Au-B 3c-2e bonds. Theoretical evidences at both density functional theory (DFT) and wave function theory levels strongly suggest that bridging Au atoms exist in the ground states of C_{2v} B_2Au^-($^1A_1$), C_2 $B_2Au_3^-$(^1A), C_{2v} B_2Au_3($^2B_1$), C_{2v} $B_2Au_5^-$($^1A_1$), and C_s B_2Au_5($^2A''$), which all contain a B—Au—B 3c-2e bond. Bridging B—Au—B units appear to be energetically favored over bridging B—H—B in $B_2H_mAu_n^-$ ($m + n = 3, 5$) mixed clusters, as demonstrated by the fact that the Au-bridged C_{2v} $B_2H_2Au^-$ ($^1A_1$), C_s $B_2HAu_2^-$ ($^1A'$), and C_1 $B_2HAu_4^-$ (^1A) lie obviously lower than their H-bridged isomers C_s $B_2H_2Au^-$ ($^1A'$), C_2 $B_2HAu_2^-$ (^1A), and C_{2v} $B_2HAu_4^-$ ($^1A_1$). The adiabatic (ADEs) and vertical

Correspondence to: S.-D. Li; e-mail: lisidian@yahoo.com

electron detachment energies (VDEs) of $B_2Au_n^-$ and $B_2H_mAu_n^-$ anions have been calculated to aid their photoelectron spectroscopy (PES) characterizations. The results achieved in this work establish an interesting 3c-2e bonding model (B—Au—B) for electron-deficient systems and present the possibilities of new gold-rich compounds, which may possess novel catalytic and chemical properties.[5–11]

Theoretical Methods

Intensive structural searches were performed using a DFT-based random structure-generating program (GXYZ).[12] Further structural optimizations, frequency analyses, and natural-localized molecular orbital (NLMO) analyses were comparatively carried out on low lying isomers using the hybrid B3LYP[13] method and the second-order Møller-Plesset approach with the frozen core approximation (MP2(FC)).[14] MP2 produced similar ground-state structures and relative energy orders with B3LYP with slightly different bond parameters. Relative energies for the lowest lying isomers were further refined using the coupled cluster method with triple excitations (CCSD(T))[15] at B3LYP structures. The Stuttgart quasi-relativistic pseudo-potentials and basis sets augmented with two f-type polarization functions and one g-type polarization function (Stuttgart_rsc_1997_ecp + 2f1g [α(f) = 0.498, α(f) = 1.464, and α(g) = 1.218)][16] were employed for Au with 19 valence electrons, and the augmented Dunning's correlation consistent basis set of aug-cc-pvTZ[17] was used for B and H throughout this work. The ADEs of the anions were calculated as the energy differences between the anions and the corresponding neutrals at their ground-state structures, whereas VDEs calculated as the energy differences between the anions and neutrals at the anionic structures. Such a theoretical procedure has proven to be reliable for $SiAu_4^-$, $Si_2Au_x^-$, and $B_7Au_2^-$ in predicting their ground-state structures and analyzing their PES spectra.[6–8] The low lying isomers obtained are depicted in Figures 1–4 with relative energies at B3LYP, MP2, and CCSD(T)//B3LYP indicated. The molecular orbital (MO) pictures, contour plots, and orbital hybridizations of the B—Au—B 3c-2e τ bonds discussed in this work are shown in Figure 5, with the natural atomic charges and Wiberg bond indexes of $B_2Au_n^{-/0}$ (n = 1, 3, 5) tabulated in Table 1 and ADEs and VDEs of the $B_2Au_n^-$ and $B_2H_mAu_n^-$ anions summarized in Table 2. All the calculations in this work were performed using the Gaussian 03 program.[18]

Results and Discussion

B_2Au^- and B_2Au

We started from B_2Au^- and B_2Au, the smallest diboron aurides possible to contain a bridging B—Au—B unit. As shown in Figure 1, the Au-bridged C_{2v} B_2Au^- ($^1A_1$) (**1**) is indeed the ground state of B_2Au^-: it lies 1.12 and 0.12 eV lower than the non-bridged C_s B_2Au^- ($^3A''$) (**2**) at MP2 and CCSD(T), respectively (though it is 0.64 eV less stable than C_s **2** at B3LYP). However, the Au-bridged C_{2v} B_2Au ($^2B_1$) neutral (**3**) proves to be a local minimum lying 0.63, 0.06, and 0.15 eV higher than the non-bridged $C_{\infty v}$ B_2Au ($^4\Sigma_g^-$) (**4**) at B3LYP, MP2, and CCSD(T), respectively. B_2Au neutral has the same number of valence electrons as B_2^- ($^4\Sigma_g^-$)[19] and $C_{\infty v}$ B_2Au (**4**) possesses the same geometry as linear B_2H.[20] In C_{2v} B_2Au^- ($^1A_1$) (**1**), Au 6s overlaps with one of the two half-filled π_u orbitals of $B_2(^3\Sigma_g^-)$[19] and the extra electron of the anion enters the other half-filled B-B π_u orbital perpendicular to the molecular plane. The bond order increase from WBI_{B-B} = 1.96 in **3** to WBI_{B-B} = 2.77 in **1**, and the bond length decrease from r_{B-B} = 1.65 Å in **3** to r_{B-B} = 1.60 Å in **1** well support this bonding mode. The natural atomic charges of q_B = −0.58 |e| and $q_{Au(b)}$ = +0.16|e| and the B-Au bridging bond orders of $WBI_{B\text{-}Au(b)}$ = 0.76 in C_{2v} B_2Au^- (**1**) also indicates that the extra electron of the anion has been totally localized between B—B, and the bridging B—Au—B 3c-2e interaction is mainly covalent.

Detailed NLMO analyses quantitatively reveal the existence of a bridging B—Au—B 3c-2e bond (τ bond) in both C_{2v} B_2Au^- (**1**) and C_{2v} B_2Au (**3**), as clearly shown in their 3c-2e orbital pictures, contour plots, and orbital hybridizations in Figure 5. With the orbital hybridization of $\tau_{B-Au-B} = 0.50(sp^{22.2})_B + 0.71(sd^{0.09})_{Au} + 0.50(sp^{22.2})_B$ and the corresponding atomic contribution of 25%B + 50%Au + 25%B for the 3c-2e bond in C_{2v} B_2Au^- (**1**), Au 6s makes 91.9% and Au 5d makes 8.0% contribution to the Au-based orbital, whereas B 2p contributes 94.8% and B 2s contributes 4.3% to the B-based orbital. Obviously, Au 6s and B 2p make the major contributions to the B—Au—B bridging bond in C_{2v} B_2Au^-. This agrees with the qualitative discussion presented earlier. However, the 8% contribution from Au 5d is not negligible due to the strong relativistic effects of Au. Thus, the 3c-2e bond of C_{2v} B_2Au^- can be practically approximated as $\tau_{B-Au-B} = 0.50(p)_B + 0.71(sd^{0.09})_{Au} + 0.50(p)_B$, as shown in Figure 5. As a local minimum, neutral C_{2v} B_2Au (**3**) possesses a similar τ_{B-Au-B} bond with C_{2v} B_2Au^-(**1**).

$B_2Au_3^-$, $B_2H_2Au^-$, and $B_2HAu_2^-$

Adding one-Au terminally to each B center in C_{2v} B_2Au^- (**1**) produces the ground state of the slightly distorted T-shaped C_2 $B_2Au_3^-$ (^1A) (**5**) (C_2 **5** has the exact symmetry of C_{2v} at MP2), which proves to be 0.35, 1.50, and 1.68 eV more stable than the Y-shaped transition state of C_s $B_2Au_3^-$ ($^1A'$) (**6**) (which has one small imaginary frequency at 15i cm^{-1} vibrationally leading to C_2 **5**), the slightly distorted chain C_s $B_2Au_3^-$ ($^1A'$) (**7**), and the slightly off-planed C_1 $B_2Au_3^-$ (^1A) (**8**) at CCSD(T), respectively. The Au-bridged C_2 $B_2Au_3^-$ (**5**) with the B—B distance of r_{B-B} = 1.53 Å is the diboron auride analogue of the H-bridged C_{2v} $B_2H_3^-$ in which r_{B-B} = 1.466 Å at MP2(full)/6-311G**.[20,21] The terminal (t) and bridging (b) bonds in C_2 $B_2Au_3^-$ (**5**) have the bond lengths of $r_{B-Au(t)}$ = 1.98 Å and $r_{B-Au(b)}$ = 2.18 Å, and the corresponding bond orders of $WBI_{B-Au(t)}$ = 1.05 and $WBI_{B-Au(b)}$ = 0.62, respectively. The atomic charges of q_B = −0.68|e|, $q_{Au(b)}$ = +0.22|e|, and $q_{Au(t)}$ = +0.07 |e|, and the B—Au bridging bond orders of $WBI_{B-Au(b)}$ = 0.62 in **5** indicate again that the extra electron of the anion is totally localized in the B—B π_u orbital perpendicular to the molecular plane, and the B—Au—B 3c-2e bond is basically covalent. Different from B_2H_3 that favors a non-bridged C_{2v} B_2H_3 ($^2B_1$) (similar to C_{2v} **26**),[21] B_2Au_3 neutral favors

(a) B_2Au^- (b) B_2Au

	1. C_{2v} ($^1A_1$)	**2**. C_s ($^3A''$)	**3**. C_{2v} ($^2B_1$)	**4**. $C_{\infty v}$ ($^4\Sigma_g^-$)
Δ**E**/B3LYP	0.00	-0.64	0.00	-0.63
MP2	0.00	+1.12	0.00	-0.06
CCSD(T)	0.00	+0.12	0.00	-0.15

Figure 1. Two Lowest lying isomers of (a) B_2Au^- and (b) B_2Au at B3LYP, with the relative energies ΔE (eV) at B3LYP//B3LYP, MP2//MP2, and CCSD(T)//B3LYP indicated.

(a) $B_2Au_3^-$

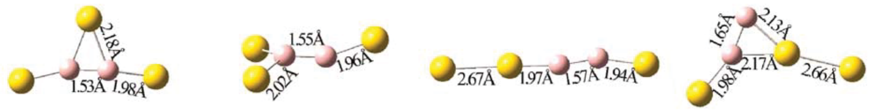

	5. C_2 (^1A)	**6**. C_s ($^1A'$)	**7**. C_s ($^1A'$)	**8**. C_1 (^1A)
Δ**E**/B3LYP	0.00	+0.17	+0.91	+1.35
MP2	0.00	+0.64	+2.38	+1.27
CCSD(T)	0.00	+0.35	+1.50	+1.68

(b) $B_2H_2Au^-$

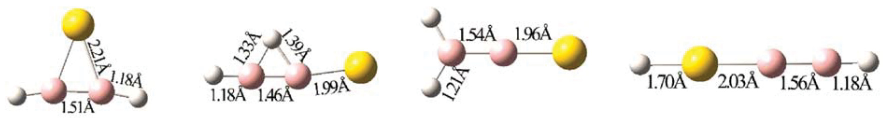

	9. C_{2v} ($^1A_1$)	**10**. C_s ($^1A'$)	**11**. C_{2v} ($^1A_1$)	**12**. C_s ($^1A'$)
Δ**E**/B3LYP	0.00	+0.53	+0.47	+1.92
MP2	0.00	+0.76	+0.99	+2.45
CCSD(T)	0.00	+0.57	+0.65	+1.91

(c) $B_2HAu_2^-$

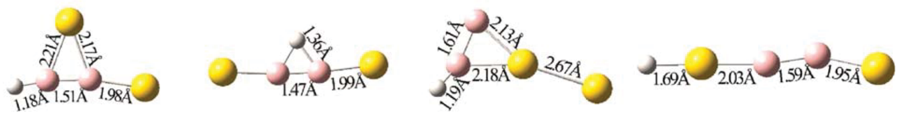

	13. C_s ($^1A'$)	**14**. C_2 (^1A)	**15**. C_1 (^1A)	**16**. C_s ($^1A'$)
Δ**E**/B3LYP	0.00	+0.62	+1.55	+1.79
MP2	0.00	+0.95	+2.45	+2.60
CCSD(T)	0.00	+0.69	+1.77	+1.89

Figure 2. Four lowest lying isomers of (a) $B_2Au_3^-$, (b) $B_2H_2Au^-$, and (c) $B_2HAu_2^-$ at B3LYP, with relative energies ΔE (eV) at B3LYP//B3LYP, MP2//MP2, and CCSD(T)//B3LYP indicated.

(a) $B_2Au_5^-$

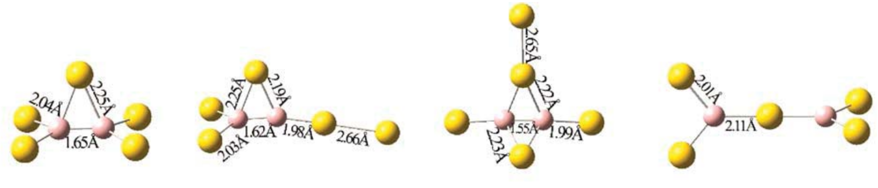

	17. C_{2v} ($^1A_1$)	18. C_s ($^1A'$)	19. C_s ($^1A'$)	20. D_{2d} ($^1A_1$)
ΔE/B3LYP	0.00	+0.01	+0.20	+0.72
MP2	0.00	+1.44	+1.64	+2.10
CCSD(T)	0.00	+0.64	+0.62	+1.42

(b) $B_2HAu_4^-$

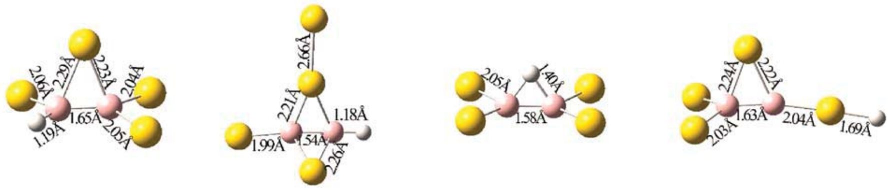

	21. C_1 (^1A)	22. C_1 (^1A)	23. C_{2v} ($^1A_1$)	24. C_s ($^1A'$)
ΔE/B3LYP	0.00	+0.06	+0.58	+0.82
MP2	0.00	+0.80	+1.01	+1.33
CCSD(T)	0.00	+0.43	+0.71	+0.88

Figure 3. Four lowest lying isomers of (a) $B_2Au_5^-$, (b) $B_2HAu_4^-$ at B3LYP, with relative energies ΔE (eV) at B3LYP//B3LYP, MP2//MP2, and CCSD(T)//B3LYP indicated.

the Au-bridged C_{2v} B_2Au_3 ($^2B_1$) (**25**), which lies 0.39 eV lower than the nonbridged C_{2v} B_2Au_3 ($^2B_1$) (**26**).

It is interesting to compare the 3c-2e bonds in the slightly distorted C_2 $B_2Au_3^-$ (**5**) [$\tau_{B-Au-B} = 0.52(p)_B + 0.67(sd^{0.06})_{Au} + 0.52(p)_B$] and C_{2v} $B_2H_3^-$ [$\tau_{B-H-B} = 0.52(sp^{8.6})_B + 0.67(s)_H + 0.52(sp^{8.6})_B$] at B3LYP level. Surprisingly, bridging Au ($sd^{0.06}$) in $B_2Au_3^-$ and bridging H (s) in $B_2H_3^-$ make exactly the same contribution (45%) to the 3c-2e interactions in these T-shaped monoanions! However, there exist obvious differences between them in orbital hybridizations. First, the 27% contribution from each B center is different: B 2s orbital in $B_2H_3^-$ makes about 10% contribution to the B sp hybridization, whereas B 2s in $B_2Au_3^-$ contributes <3%, which has been omitted in Figure 5. Second, the Au-based orbital in $B_2Au_3^-$ contains 94.2% contribution from Au 6s

(a) B_2Au_3

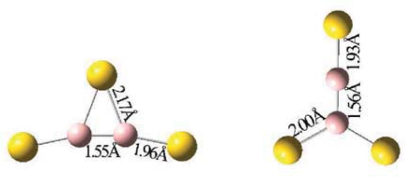

(b) B_2Au_5

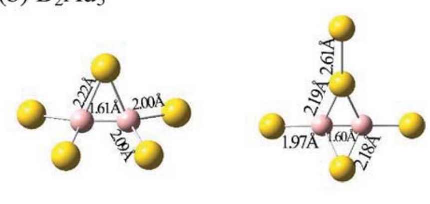

	25. C_{2v} ($^2B_1$)	26. C_{2v} ($^2B_1$)	27. C_s ($^2A''$)	28. C_s ($^2A''$)
ΔE/B3LYP	0.00	+0.21	0.00	+0.28
MP2	0.00	+0.59	0.00	+1.30
CCSD(T)	0.00	+0.39	0.00	+0.85

Figure 4. Two lowest lying isomers of (a) B_2Au_3 and (b) B_2Au_5 neutrals obtained at B3LYP, with relative energies ΔE (eV) at B3LYP//B3LYP, MP2//MP2, and CCSD(T)//B3LYP indicated.

Table 1. Calculated Natural Atomic Charges (q/|e|), Wiberg Bond Indexes (WBI), and Total Atomic Bond Orders (WBI_B and WBI_{Au}) of the Au-bridged $B_2Au_n^{-/0}$ Clusters at B3LYP Level. Au(t) and Au(b) represent terminal and bridging Au atoms, respectively.

	q_B	$q_{Au(t)}$	$q_{Au(b)}$	WBI		WBI_B	$WBI_{Au(b)}$
C_{2v} B_2Au^-(**1**)	−0.58		0.16	B—B	2.77	3.54	1.52
				B—Au(b)	0.76		
C_{2v} B_2Au(**3**)	−0.15		0.29	B—B	1.96	2.70	1.49
				B—Au(b)	0.74		
C_2 $B_2Au_3^-$(**5**)	−0.68	0.07	0.22	B—B	2.15	3.89	1.34
				B—Au(b)	0.62		
				B—Au(t)	1.05		
C_{2v} B_2Au_3(**25**)	−0.36	0.21	0.31	B—B	1.54	3.30	1.34
				B—Au(b)	0.62		
				B—Au(t)	1.11		
C_{2v} $B_2Au_5^-$(**17**)	−0.73	0.06	0.24	B—B	1.40	3.99	1.30
				B—Au(b)	0.56		
				B—Au(t)	0.98		
C_s B_2Au_5(**27**)	−0.75	0.30, 0.27	0.35	B—B	1.46	3.85	1.30
				B—Au(b)	0.57		
				B—Au(t)	0.95, 0.74		

and 5.8% from Au 5d, whereas the H-based orbital in $B_2H_3^-$ contains contribution purely from H 1s.

As typical diboron mixed clusters, $B_2H_2Au^-$ and $B_2HAu_2^-$ provide two good candidates to compare bridging B—Au—B interaction with bridging B—H—B in one molecule. As shown in Figures 2b and 2c, at CCSD(T) level, the Au-bridged C_{2v} $B_2H_2Au^-$ ($^1A'$) (**9**) is 0.57 eV more stable than the H-bridged C_s $B_2H_2Au^-$ ($^1A'$) (**10**), with C_{2v} $B_2H_2Au^-$ ($^1A_1$) (**11**) and C_s $B_2H_2Au^-$ ($^1A'$) (**12**) lying 0.65 eV and 1.91 eV higher than C_{2v} **9**, respectively. Similarly, the Au-bridged C_s $B_2HAu_2^-$ ($^1A'$) (**13**) lies 0.69 eV lower than the H-bridged C_2 $B_2HAu_2^-$ (^1A) (**14**), with C_1 $B_2HAu_2^-$ (^1A) (**15**) and C_s $B_2HAu_2^-$ ($^1A'$) (**16**) lying 1.77 and 1.89 eV above the ground state. The bridging B—Au—B 3c-2e bonds in C_{2v} $B_2H_2Au^-$ (**9**) and C_s $B_2HAu_2^-$ (**13**) possess the orbital hybridizations of $\tau_{B-Au-B} = 0.49(p)_B + 0.72(sd^{0.09})_{Au} + 0.49(p)_B$ and $\tau_{B-Au-B} = 0.48(p)_{B'} + 0.69(sd^{0.08})_{Au} + 0.54(p)_B$ (B′ stands for the B atom connected to terminal H), respectively. Similar to C_2 $B_2Au_3^-$ (^1A) (**5**), both C_{2v} **9** and C_s **13** contain a B=B double bond ($\sigma + \pi$) with the approximate bond lengths of $r_{B-B} = 1.51$ Å. The high stability of bridging B—Au—B over bridging B—H—B in these mixed anions can be understood considering the fact that the bridging Au ($6s5d^{0.08-0.09}$) is much bigger than bridging H (1s) in orbital size and, therefore, better overlaps with the p-p π_u orbital of the B—B unit (with major contribution coming from the Au $5d_{x2-y2}$ orbital in B—B direction). The p-π character of the 3c-2e bonds in diboron auride clusters and mixed analogues can be clearly seen from their orbital pictures and contour plots, which all contain effective p-p overlaps on the opposite sides of the bridging B—Au—B triangles, as shown in Figure 5.

It is interesting to notice that our calculation produces nearly the same B—B bond lengths for the Au-bridged C_2 $B_2Au_3^-$ (**5**) ($r_{B-B} = 1.53$ Å) and the unbridged C_s $B_2Au_3^-$ (**6**) ($r_{B-B} = 1.55$ Å), whereas for the corresponding boron hydride of $B_2H_3^-$, the H-bridged B—B bond ($r_{B-B} = 1.46$ Å) in the ground state C_{2v} $B_2H_3^-$ (similar to C_2 **5**) was obviously shorter than the unbridged B—B ($r_{B-B} = 1.56$ Å) in a C_{2v} local minimum (analogous to C_s **6**).[20,21] This situation can be qualitatively explained in terms of the atomic size difference between Au and H: a bridging Au (6s5d) is much bigger than a bridging H(1s) in size, and therefore, to form a stable B—Au—B bridge in C_2 $B_2Au_3^-$ (**5**), the B—B bond is obviously elongated by about 0.07 Å to reduce the geometrical strains. This B—B bond length elongation agrees with the Wiberg bond order decreasing from WBI = 2.29 in the H-bridged C_{2v} $B_2H_3^-$ ($^1A_1$) to WBI = 2.15 in the Au-bridged C_2 $B_2Au_3^-$ (^1A). As indicated in Figure 2, the calculated B—B distances in the Au-bridged C_{2v} **9** (1.51 Å) and C_s **13** (1.51 Å), all prove to be obviously longer than B—B distances in the corresponding H-bridged C_s **10** (1.46 Å) and C_2 **14** (1.47 Å), respectively, well in line with the fact that the

Table 2. Calculated ADEs (eV) and VDEs (eV) of the Diboron Auride Anions and Mixed Analogues at B3LYP and CCSD(T)//B3LYP Levels. ADEs of the anions are equivalent to the electron affinities of the corresponding neutrals.

	ADE		VDE	
	B3LYP	CCSD(T)	B3LYP	CCSD(T)
C_{2v} B_2Au^-($^1A_1$)	1.68($^2B_1$)	1.74($^2B_1$)	1.70($^2B_1$)	1.77($^2B_1$)
C_2 $B_2Au_3^-$(^1A)	1.72($^2B_1$)[a]	1.74($^2B_1$)[a]	1.81(^2B)	1.89(^2B)
C_{2v} $B_2H_2Au^-$($^1A_1$)	1.47($^2B_1$)	1.50($^2B_1$)	1.49($^2B_1$)	1.55($^2B_1$)
C_s $B_2HAu_2^-$($^1A'$)	1.61($^2A''$)	1.65($^2A''$)	1.64($^2A''$)	1.70($^2A''$)
C_{2v} $B_2Au_5^-$($^1A_1$)	2.98($^2A''$)[b]	2.86($^2A''$)[b]	3.23($^2A_2$)	3.36($^2A_2$)
C_1 $B_2HAu_4^-$(^1A)[c]	2.99(^2A)		3.39(^2A)	

[a]The final state corresponds to C_{2v} B_2Au_3($^2B_1$)(**25**).
[b]The final state corresponds to C_s B_2Au_5($^2A''$)(**27**).
[c]CCSD(T) calculations on doublet C_1 B_2HAu_4 neutrals are beyond the reach of available computing resources.

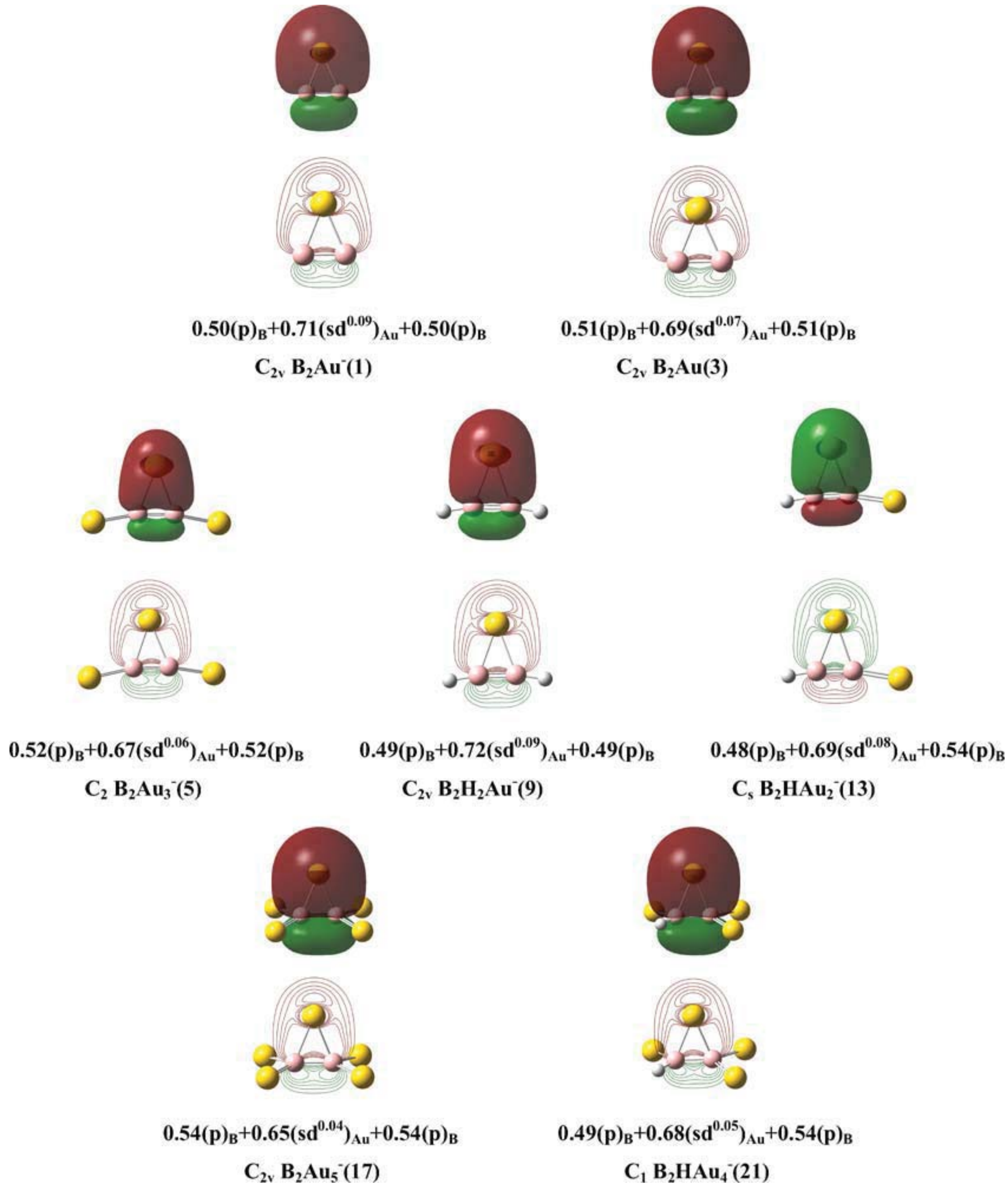

Figure 5. Three-dimensional views, contour plots, and orbital hybridizations of the 3c-2e τ bonds in B_2Au^-(**1**), B_2Au(**3**), $B_2Au_3^-$(**5**), $B_2H_2Au^-$(**9**), $B_2HAu_2^-$(**13**), $B_2Au_5^-$(**17**), and $B_2HAu_4^-$(**21**) discussed in this work. [Color figure can be viewed in the online issue, which is available at wileyonlinelibrary.com.]

Wiberg bond orders of C_{2v} **9** (2.16) and C_s **13** (2.17) are systematically lower than that of Cs **10** (2.24) and C_2 **14** (2.20). On the other hand, an —Au terminal proves to cause only minor changes to the attached B—B units in bond lengths, as shown in the typical cases of the Au-terminated C_s **7** and C_s **16,** which have very similar B—B bond lengths with the H-terminated B—B bond in C_s **12**. The two factors work together to make the B—B bond length in the bridged C_2 $B_2Au_3^-$ (**5**) only slightly shorter than B—B bond in the unbridged C_s $B_2Au_3^-$ (**6**). Similar situations happen to the Au-bridged B_2Au^- discussed earlier and $B_2Au_5^-$ detailed in the next section. The B3LYP results obtained above well parallel the results previously reported for the corresponding boron hydrides[20–23] and invite experimental and more accurate theoretical confirmations.

$B_2Au_5^-$ and $B_2HAu_4^-$

We now turn to $B_2Au_5^-$ and its mixed analogue $B_2HAu_4^-$. $B_2Au_5^-$ has the high-symmetry ground state of the Au-bridged C_{2v} $B_2Au_5^-$ ($^1A_1$) (**17**) that lies 0.64, 0.62, and 1.42 eV lower than C_s $B_2Au_5^-$($^1A'$) (**18**), C_s $B_2Au_5^-$($^1A'$) (**19**), and D_{2d} $B_2Au_5^-$ ($^1A_1$) (**20**) at CCSD(T), respectively. C_{2v} $B_2Au_5^-$ (**17**) is the diboron auride analogue of the H-bridged C_{2v} $B_2H_5^-$[22] The τ_{B-Au-B} bond in C_{2v} $B_2Au_5^-$ possesses the orbital hybridization of $\tau_{B-Au-B} = 0.54(p)_B + 0.65(sd^{0.04})_{Au} + 0.54(p)_B$. The two sp^2-hybridized B atoms in C_{2v} $B_2Au_5^-$ form a B—B σ bond with $r_{B-B} = 1.65$ Å in the Au_2B-BAu_2 plane, whereas the Au $6s^1$ electron and the extra electron of the anion form the bridging B—Au—B 3c-2e interaction with $r_{B-Au}(b) = 2.25$ Å. Similar to the H-bridged C_{2v} B_2H_5,[20,23] B_2Au_5 neutral favors the Au-bridged C_s B_2Au_5 ($^2A''$) (**27**) over the slightly off-planed C_s B_2Au_5 ($^2A''$) (**28**) by 0.85 eV. It is interesting to notice that that bridging Au atoms in the whole $B_2Au_n^{-/0}$ series ($n = 1, 3, 5$) have considerably high total bond orders between $WBI_{Au(b)} = 1.30$–1.52 (Table 1), indicating that effective multi-center interactions (3c-2e) exist in these diboron auride clusters. Similar situation exists in their mixed analogues.

The Au-bridged C_1 $B_2HAu_4^-$ (^1A) (**21**) appears to lie 0.71 eV lower than the H-bridged C_{2v} $B_2HAu_4^-$ ($^1A_1$) (**23**) and 0.43 eV and 0.88 eV lower than C_1 $B_2HAu_4^-$ (^1A) (**22**) and C_s $B_2HAu_4^-$ ($^1A'$) (**24**) at CCSD(T), respectively, indicating again that a bridging B—Au—B unit is favored over a bridging B—H—B in mixed anions. With two unsymmetrical B centers, C_1 $B_2HAu_4^-$ (**21**) with $r_{B'-B} = 1.65$Å possesses the 3c-2e bond of $\tau_{B-Au-B'} = 0.49(p)_{B'} + 0.68(sd^{0.05})_{Au} + 0.54(p)_B$. There exists a general trend to notice that, in the orbital hybridizations of the 3c-2e bonds shown in Figure 5, the B′ centers directly connected to H-terminals have slightly lower orbital coefficients (0.48–0.49) and, therefore, less contribution to the multi-center interactions than B centers directly bonded to Au-terminals (0.50–0.54).

Thermodynamic Stabilities and Electron Detachment Energies

Concerning the thermodynamic stabilities of the diboron auride clusters studied in this work, at CCSD(T)//B3LYP level, we calculate the atomization energies (AEs) of the low lying B_2Au_n neutral isomers compared with that of the corresponding B_2H_n ($n = 1, 3, 5$)[20,23]

$$B_2Au(C_{\infty v},{}^4\Sigma_g^-)(\mathbf{4}) = 2B(^2P) + Au(^2S) \qquad \Delta E = 153.4\ \text{kcal/mol}$$
$$B_2H(C_{\infty v},{}^4\Sigma_g^-) = 2B(^2P) + H(^2S) \qquad \Delta E = 167.9\ \text{kcal/mol}$$
$$B_2Au_3(C_{2v},{}^2B_1)(\mathbf{26}) = 2B(^2P) + 3Au(^2S) \qquad \Delta E = 319.8\ \text{kcal/mol}$$
$$B_2H_3(C_{2v},{}^2B_1) = 2B(^2P) + 3H(^2S) \qquad \Delta E = 351.8\ \text{kcal/mol}$$
$$B_2Au_5(C_s,{}^2A'')(\mathbf{27}) = 2B(^2P) + 5Au(^2S) \qquad \Delta E = 463.1\ \text{kcal/mol}$$
$$B_2H_5(C_{2v},{}^2A_1) = 2B(^2P) + 5H(^2S) \qquad \Delta E = 490.7\ \text{kcal/mol}$$

and the fragmentation energies (FEs) required to remove an Au^- anion or Au atom from $B_2Au_n^-$ ($n = 1,3,5$) in the following processes

$$B_2Au^-(C_{2v},{}^1A_1)(\mathbf{1}) = B_2(^3\Sigma_g^-) + Au^-(^1S) \qquad \Delta E = 81.2\ \text{kcal/mol}$$
$$B_2Au^-(C_{2v},{}^1A_1)(\mathbf{1}) = B_2^-(^4\Sigma_g^-) + Au(^2S) \qquad \Delta E = 83.0\ \text{kcal/mol}$$
$$B_2Au_3^-(C_2,{}^1A)(\mathbf{5}) = B_2Au_2(D_{\infty h},{}^3\Sigma_g^-) + Au^-(^1S) \qquad \Delta E = 77.1\ \text{kcal/mol}$$
$$B_2Au_3^-(C_2,{}^1A)(\mathbf{5}) = B_2Au_2^-(C_{2h},{}^2A_u) + Au^-(^2S) \qquad \Delta E = 89.4\ \text{kcal/mol}$$
$$B_2Au_5^-(C_{2v},{}^1A_1)(\mathbf{17}) = B_2Au_4(D_{2d},{}^1A_1) + Au^-(^1S) \qquad \Delta E = 79.1\ \text{kcal/mol}$$
$$B_2Au_5^-(C_{2v},{}^1A_1)(\mathbf{17}) = B_2Au_4^-(D_2,{}^2B_3) + Au(^2S) \qquad \Delta E = 87.7\ \text{kcal/mol}$$

in which the linear $D_{\infty h}$ $B_2Au_2(^3\Sigma g^-)$, zigzag C_{2h} $B_2Au_2^-(^2A_u)$, the staggered D_{2d} $B_2Au_4(^1A_1)$, and the slightly distorted ethylene-like D_2 $B_2Au_4^-(^2B_3)$ are the lowest energy isomers obtained for the corresponding fragments. As shown above, AE = 153.4 kcal/mol for $C_{\infty v}$ B_2Au(**4**), 319.8 kcal/mol for C_{2v} B_2Au_3(**26**), and 463.1 kcal/mol for C_{2v} B_2Au_5 (**27**). According to the relative energies calculated at CCSD(T), AE = 149.9 kcal/mol for C_{2v} B_2Au(**3**) and 328.8 kcal/mol for C_{2v} B_2Au_3(**25**). These AEs appear to be comparable (though systematically lower by 5∼10%) with the corresponding values of diboron hydrides B_2H_n($n = 1,3,5$) at the same theoretical level, suggesting that B_2Au_n clusters be thermodynamically stable. Removing the bridging Au of the ground state $B_2Au_n^-$ anions (Figs. 1–3) to produce an Au^- plus a B_2Au_{n-1} neutral prove to have the lowest fragmentation energies in various processes, with FE = 81.2 kcal/mol for C_{2v} B_2Au^- (**1**), 77.1 kcal/mol for C_2 $B_2Au_3^-$ (**5**), and 79.1 kcal/mol for C_{2v} B_2Au_5 (**17**). Fragmentations in $B_2Au_3^-(C_2,{}^1A)$ = $B_2(^3\Sigma_g^-)$+$Au_3^-(D_{\infty h},{}^1\Sigma_g^+)$ with FE = 146.0 kcal/mol, $B_2Au_5^-(C_{2v},{}^1A_1)$ = $B_2(^3\Sigma_g^-)$+$Au_5^-(C_{2v},{}^1A_1)$ with FE = 199.5 kcal/mol, and other processes involving the breakdown of B—B bonds appear to be much less favorable in energies.

We also calculate the ADE and VDE values of the anions possible to be measured in PES experiments. As can be seen from Table 2, B3LYP and CCSD(T)//B3LYP methods agree well in producing the one-electron detachment energies of these anions. For $B_2H_mAu_n^-$ with $m + n = 1$ and 3, the calculated ADEs and VDEs lie between 1.47 and 1.89 eV, whereas for $m + n = 5$, the corresponding values seem to be obviously higher (2.86–3.39 eV). The high-electron detachment energies of $B_2Au_5^-$ and $B_2HAu_4^-$ anions may be related with the fact that they have the same number of valence electrons as the well-known diborane B_2H_6. The electron binding energies of these anions fall within the energy range of the conventional excitation laser (266 nm, 4.661 eV) in PES measurements.[6–8]

Summary

Ab initio theoretical evidences obtained in this work strongly suggest that bridging gold atoms exist in diboron aurides $B_2Au_n^{-/0}$ (n = 1, 3, 5) and their $B_2H_mAu_n^-$ mixed analogues ($m + n$ = 3, 5) that all prove to possess a B—Au—B 3c-2e bond. Bridging B—Au—B units appear to be favored in energy over B—H—B in mixed clusters. B—B units with the B—B distances of 1.46–1.68 Å are well maintained in most of the low lying isomers obtained in this work (except D_{2d} **20**). Detailed orbital analyses indicate that Au 6s makes 92–96% and Au 5d makes 8–4% contribution to the Au-based orbitals in bridging B—Au—B units, partially reflecting the relativistic effect of gold. Diboron auride clusters and their mixed analogues are thermodynamically stable and possible to be produced by laser ablation of B—Au binary targets and characterized with PES spectra. The concept of B—Au—B 3c-2e bonds proposed in this work provides an interesting bonding mode for electron-deficient systems and helps to design new materials and catalysts with highly dispersed Au atoms.[6–9] Initial investigations indicate that both the double Au-bridged D_{2h} B_2Au_6 and D_{2h} $B_2Au_6^-$ similar to the double H-bridged D_{2h} B_2H_6 are true minima of the systems and $Al_2Au_n^{-/0}$ and $Ga_2Au_n^{-/0}$ clusters (n = 1–6) possess certain similarities and differences with $B_2Au_n^{-/0}$.

References

1. Pyykko P. Angew Chem Int Ed 2002, 41, 3573 and references therein.
2. Cotton F. A.; Wikinson G.; Murillo C. A.; Bochmann M. Advanced Inorganic Chemistry, 6th ed., Wiley: New York, 1999.
3. Schwarz H. Angew Chem Int Ed 2003, 42, 4442 and references therein.
4. Gagliardi L. J Am Chem Soc 2003, 125 7504.
5. (a) Hall K. P.; Mingos D. M. P. Prog Inorg Chem 1984, 32 237; (b) Lauher J. W.; Wald K. J Am Chem Soc 1981, 103, 7648; (c) Burdett J. K.; Eisentein O.; Schweizer W. B. Inorg Chem 1994, 33, 3261.
6. Kiran B.; Li X.; Zhai H.-J.; Cui L.-F.; Wang L.-S. Angew Chem Int Ed 2004, 43, 2125.
7. (a) Li X.; Kiran B.; Wang L.-S. J Phys Chem A 2005, 109, 4366; (b) Kiran B.; Li X.; Zhai H.-J.; Wang L.-S. J Chem Phys 2006, 125, 133204.
8. Zhai H.-J.; Wang L.-S.; Zubarev D. Y.; Boldyrev A. I. J Phys Chem A 2006, 110, 1689.
9. Zubarev D. Y.; Li J.; Wang L.-S.; Boldyrev A.-I. Inorg Chem 2006, 45, 5269.
10. Pyykko P.; Zhao Y. Chem Phys Lett 1991, 117, 103.
11. Avramopoulos A.; Papadopoulos M. G.; Sadlej A. J Chem Phys Lett 2003, 370, 765.
12. Lu, H.-G. In GXYZ Ver. 1.0, A Random Cartesian Coordinates Generating Program, Shanxi University: Taiyuan, 2008.
13. (a) Becke A. D. J Chem Phys 1993, 98, 5648; (b) Lee C.; Yang W.; Parr R. G. Phys Rev B 1988, 37, 785.
14. (a) Head-Gordon M.; Pople J. A.; Frisch, M. J. Chem Phys Lett 1988, 153, 503; (b) Frisch M. J.; Head-Gordon M.; Pople J. A. Chem Phys Lett 1990, 166, 275; (c) Frisch M. J.; Head-Gordon M.; Pople J. A. Chem Phys Lett 1990, 166, 281; (d) Head-Gordon M.; Head -Gordon T. Chem Phys Lett 1994, 220, 122; (e) Saebo S.; Almlof J. Chem Phys Lett 1989, 154, 83.
15. (a) Cizek J. Adv Chem Phys 1969, 14, 35; (b) Scuseria G. E.; Schaefer H. F. J Chem Phys 1989, 90, 3700; (c) Pople J. A.; Head-Gordon M.; Raghavachari K. J Chem Phys 1987, 87, 5968.
16. (a) Dolg M.; Wedig U.; Stoll H.; Preuss, H. J. Chem Phys 1987, 86, 866; (b) Martin J. M. L.; Sundermann A. J Chem Phys 2001, 114, 3408.
17. Kendall R. A.; Dunning T. H.; Harrison R. J. J Chem Phys 1992, 96 6796.
18. Frisch M. J. et al. Gaussian 03, revision, A.1; Gaussian, Inc.: Pittsburgh, PA, 2003.
19. Alexandrova A. N.; Boldyrev A. I.; Zhai H.-J.; Wang L.-S. Coord Chem Rev 2006, 250, 2811.
20. Liu J.; Aeschleman J.; Rajan L. M.; Che C.; Ge Q. In Materials Issues in a Hydrogen Economy; Jena P.; Kandalam A.; Sun Q., Eds.; World Scientific Publishing Co. Ptc. Ltd: Singapore; 2009, pp. 234.
21. (a) Lammertsma K.; Ohwada T. J Am Chem Soc 1996, 118, 7247; (b) Krempp M.; Damrauer R.; DePuy C. H.; Keheyan Y. J Am Chem Soc 1994, 116, 3629; (c) Qu Z.-W.; Li Z.-S.; Ding Y.-H.; Sun C.-C. J Phys Chem A 2000, 104, 11952.
22. Sun Y.-B.; Li Z.-S.; Huang X.-R.; Sun C.-C. Chem J Chinese Universities 2002, 23, 1542.
23. (a) Longenecker J. G.; Mebel A. M.; Kaiser R. I.; Inorg Chem 2007, 46, 5739; (b) Trachtman M.; Bock C. W.; Niki H.; Mains G. J. Struct Chem 1990, 1, 171; (c) Ruscic B.; Schwarz M.; Berkowitz J. J Chem Phys 1989, 91, 4183.